minerals

MDPI

Article

Studies on Recovery of Valuable Metals by Leaching Lead–Zinc Smelting Waste with Sulfuric Acid

Chunfu Xin [1,2,3,4], Hongying Xia [1,2,3,4,*], Guiyu Jiang [1,2,3,4], Qi Zhang [1,2,3,4], Libo Zhang [1,2,3,4,*] and Yingjie Xu [1,2,3,4]

1 Faculty of Metallurgical and Energy Engineering, Kunming University of Science and Technology, Kunming 650093, China
2 State Key Laboratory of Complex Nonferrous Metal Resources Clean Utilization, Kunming University of Science and Technology, Kunming 650093, China
3 Kunming Key Laboratory of Special Metallurgy, Kunming University of Science and Technology, Kunming 650093, China
4 Key Laboratory of Unconventional Metallurgy, Ministry of Education, Kunming 650093, China
* Correspondence: hyxia@kust.edu.cn (H.X.); libozhang77@163.com (L.Z.)

Abstract: Germanium-containing residues (GCR) are a secondary resource rich in zinc (Zn) and germanium (Ge) produced in the Zn pyrometallurgical process and an important raw material for recovering Zn and Ge. To recycle the residue by hydrometallurgy, sulfuric acid is used to leach the residue under normal pressure. In this study, the experimental conditions (leaching temperature, leaching time, liquid/solid (L/S) mass ratio and initial acidity) were optimized through the experimental design to make the optimized experimental conditions consistent with the current industrial production conditions, so as to maximize the leaching rate of Zn and Ge, and the main reasons for the low leaching rate of germanium were analyzed. The results show that the optimum reaction conditions are as follows: initial acidity 160 g·L^{-1}, leaching temperature 90 °C, L/S mass ratio 5:1, leaching time 60 min and stirring speed 400 r·min^{-1}. Under the optimum reaction conditions, the leaching rates of Zn and Ge are 83.22% and 77.29%, respectively. The reason for the low leaching rates of Zn and Ge in GCR was obtained through atmospheric leaching experiment, electron probe microanalysis (EPMA), scanning electron microscopy (SEM) and energy dispersive spectroscopy (EDS), X-ray diffraction (XRD) and chemical phase analysis. GCR is mainly composed of phases such as zincite (ZnO), galena (PbS), wurtzite (ZnS) and anglesite ($PbSO_4$), and the main elements are Zn, lead (Pb), germanium (Ge), oxygen (O), sulfur (S), silicon (Si), aluminum (Al) and Fe. This study can provide a certain reference value for researchers, in order to provide a reference for the large-scale recycling of Zn and Ge resources in the future.

Keywords: germanium; zinc; germanium-containing residues; sulfuric-acid leaching; recovery; zinc smelting residue

Citation: Xin, C.; Xia, H.; Jiang, G.; Zhang, Q.; Zhang, L.; Xu, Y. Studies on Recovery of Valuable Metals by Leaching Lead–Zinc Smelting Waste with Sulfuric Acid. *Minerals* **2022**, *12*, 1200. https://doi.org/10.3390/min12101200

Academic Editors: Álvaro Aracena Caipa and Hyunjung Kim

Received: 14 August 2022
Accepted: 21 September 2022
Published: 23 September 2022

1. Introduction

Ge is an important and scarce associated resource, which has a wide and important application in semiconductors, biomedicine, aerospace, optical fiber communications, electronic equipment, photocells and other fields. The United States, Japan and China have listed it as a strategic reserve resource. Germanium is a critical raw material. Europe defines raw materials as critical raw materials mainly according to two criteria: their economic importance for European industry and their supply risk, that is, the risk of interruptions in the supply to Europe [1]. Germanium is of great significance to the development of a national economy, military and science and technology [2–4]. There are clear global trends and tendencies showing that the demand for Ge will increase dramatically in the near future.

Independent Ge deposits are rare in nature. Ge is mainly associated with other metal minerals. Therefore, Ge is mainly recovered from some Ge-rich coal seams and Pb–Zn metallurgical by-products [5–7]. China is the largest producer of most of the critical raw materials, including the rare earth elements, magnesium, tungsten, antimony, gallium and Ge. The Zn sulfide concentrate produced from Pb–Zn ore in southern China is rich in Ge. The hydrometallurgy of Zn process is the main method for extracting metallic Zn from Zn sulfide concentrate. In neutral leaching and weak acid leaching stages, sphalerite and Zn ferrite are difficult to effectively leach, and the important element Ge is not leached, almost all of them are enriched into Zn leaching residue [8,9]. With the gradual depletion of sulfide ore, valuable metals are recovered from various waste resources such as dust, scum, and waste residues in the metallurgical industry, and the world is paying more and more attention to these waste resources [10–14]. The content of Zn and Ge in Zn leaching residue is low, so Ge enrichment should be considered in the industrial extraction of Ge. Rotary kiln volatilization and fuming furnace volatilization are widely used in Ge-rich treatment of Zn leaching residue [15]. The main chemical components of GCR are Zn, Pb, S, Fe, As, Ge and Si, with special attention to the Ge content as high as 500–1000 g/t. Zn sulfide in the residue is reduced to Zn powder, and Zn powder is oxidized to Zn oxide. Therefore, the Zn-containing phases in the GCR are ZnO and ZnS, and the GCR phases are Ge oxide (GeO) and Ge dioxide (GeO_2) [16–20]. Therefore, Zn and Ge in GCR have high recovery values [21–26].

At present, sulfuric acid leaching is the most widely used industrial method to treat GCR [27–29]. The leaching residue is sent to fire to recover Pb and Ag. The leaching solution is used to precipitate Ge with tannic acid to produce Ge residue, which is burned to get Ge concentrate. After neutralization and Fe removal, the solution is sent to purification and electrolysis to extract Zn [30]. However, when using atmospheric leaching of germanium in the GCR, the leaching rate is only 70%–80%. The main reason for the low Ge leaching rate caused by the leaching of GCR by atmospheric methods has not yet been clearly explained, which leads to the lack of suitable industrial methods to solve this problem in industrial production.

In this study, the GCR was produced in the process of fuming Zn leaching residue from a Pb and Zn smelter in Yunnan Province. The company adopts the most widely used sulfuric acid leaching process and tannic acid to precipitate Ge and recover Zn and Ge from Ge-containing GCR. To study the best conditions for the treatment of GCR by atmospheric leaching process, and to find out the main reason for the low leaching rate of Zn and Ge, an atmospheric leaching test was carried out on GCR. The main reasons for the low leaching rate of Zn and Ge were analyzed by means of chemical phase analysis, X-Ray Fluorescence Spectrometer (XRF), Inductively Coupled Plasma Optical Emission Spectrometer (ICP-OES), Electron Microprobe (EPMA), X-ray powder diffraction (XRD) and Scanning Electron Microscope–Energy Dispersive Spectrometer (SEM-EDS).

2. Experiments

2.1. Materials and Methods

The raw material GCR used in the experiments was provided by a company in Yunnan, China. The samples were dried for 24 h at 105 ± 5 °C in an oven for the removal of moisture. After the material was pulverized to a particle size of 0.075 mm, the subsequent acid leaching experiment was carried out. All reagents used in this article are analytical-grade products manufactured by Chengdu Kelong Chemical Co., Ltd., Qionglai City, Sichuan Province, China. The leaching solution was prepared with deionized water.

2.2. Leaching Experiment

The schematic diagram of the leaching experiment device is shown in Figure 1. All experiments in this study were completed in 250 ml flasks (Gongyi Yuhua Instrument Co., Ltd., Zhengzhou, China). First, weigh 30 g of materials for use. Add a certain concentration of sulfuric acid solution to the flask according to the L/S mass ratio (4–8:1), and turn on the

constant temperature heating magnetic stirrer (DF-101S, Sichuan ShuBo (Group) Co., Ltd., Chongzhou, China) to heat the solution. A condensation reflux pipe was installed at the flask mouth to prevent evaporation of the solution and insert a thermometer. The mouth of the flask is sealed with a rubber stopper to prevent evaporation. The actual temperature of the solution is measured by a thermometer inserted into the flask, and the temperature range is 0–100 °C. After the sulfuric acid solution is heated to a predetermined temperature, the weighed GCR is slowly added to the leaching solution. Then turn on the magnetic stirring function of the magnetic stirrer, and stir GCR and sulfuric acid solution for a certain time. After the leaching reaction, the filter residue and filtrate were obtained by liquid–solid separation (Filter: SHZ-D (III), Tianjin Huaxin Instrument Factory, Beijing, China). The leaching residue was washed and dried to characterize, and the leaching solution was tested for the content of Zn and Ge in the solution (Drying oven: DHG-9030A, Shanghai Yiheng Scientific Instrument Co., Ltd., Shanghai, China). Each group of experiments was repeated three times under the same reaction conditions, and the average value was taken.

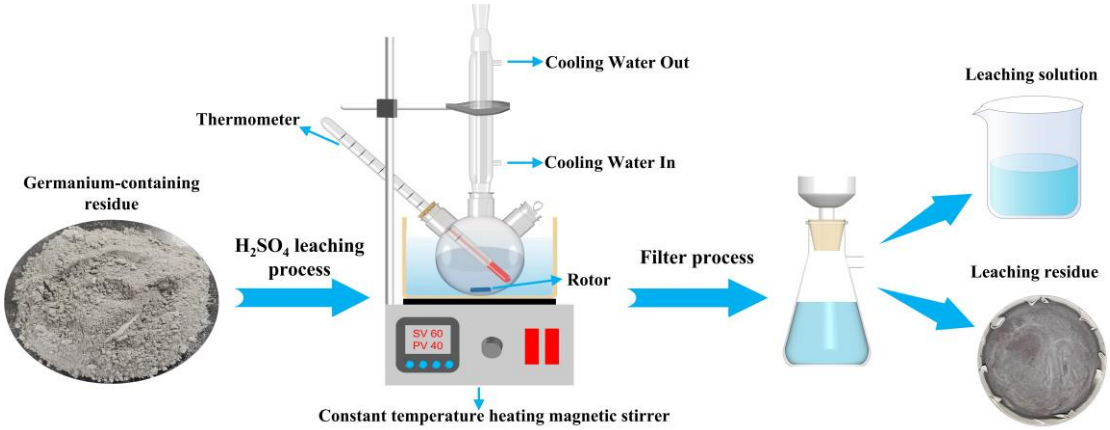

Figure 1. Schematic diagram of the leaching experimental setup.

2.3. Analytical Methods

X-ray fluorescence spectroscopy (XRF, PANalytical Axios, PANalytical B.V., Almelo, Netherlands) and X-ray powder diffraction (XRD, Philips pw1825, PHILIPS, Eindhoven, Netherlands) were used to determine the main components and phase compositions of the materials. The composition and content of Zn-containing phases were determined by chemical phase analysis. The samples were analyzed by scanning electron microscope (Nova-NanoSEM-450, FEI, Hillsboro, USA) and EPMA-1720 series electron microprobes, which provided the microstructure, mineralogy information and elemental distribution of the samples. The metal content of the samples in the solution was determined using ICP-OES (PlasmaQuant PQ9000, Analytik Jena, Jena, Germany). During the experiment, the Origin software was used to plot and analyze the data, and the Jade software was used to analyze the phase. The leaching rate (λ_{Me}) was calculated according to the following Equation (1) [31,32]:

$$\lambda_{Me} = \frac{\theta_{Me} \times V}{\theta^0_{Me} \times m} \quad (1)$$

where $\theta_{Me}(g \cdot L^{-1})$ is the concentration of Zn or Ge in the filtrate, V(L) is the volume of the filtrate, $\theta_{Me}{}^0(\%)$ is the mass fraction of Zn or Ge in the sample before acid leaching, and m(g) is the weight of the sample.

3. Results and Discussion

3.1. Characterization of the GCR

Due to the different production processes and raw materials of different Pb–Zn smelting enterprises, the properties of GCR are also different, but the main phases are ZnO, ZnS, $ZnFe_2O_4$, $PbSO_4$, PbS, GeO, $(Fe,Ge)_2O_4$ and GeO_2. Table 1 lists the XRF quantitative

analysis results of the GCR [33]. According to our previous research, the Zn-containing phases of GCR samples are mainly composed of ZnO, ZnS, $ZnSO_4$ and $ZnFe_2O_4$, and the composition structure is shown in Table 2 [33]. The XRD results of GCR were shown in Figure 2 [33]. Because the XRD instrument cannot detect the phase with low content or poor crystallinity, only four phases with high content appear as diffraction peaks, which are ZnO, ZnS, PbS and $PbSO_4$. Sulfide (such as ZnS and PbS) in the sample is difficult to be dissolved in sulfuric acid solution without oxidant.

Table 1. XRF results of the GCR.

Element	Zn	Pb	S	Fe	As	K	Si	Cd	Ag	Ge	Others (e.g., O)
Content, wt.%	49. 65	15.92	4.70	3.02	0.99	0.66	0.58	0.48	314.8 g/t	620.4 g/t	23.90

Table 2. Chemical phase analysis results of Zn in GCR.

Phase	ZnO	ZnS	$ZnSO_4$	$ZnFe_2O_4$	Total
Zn content, wt.%	42.66	5.31	0.92	0.76	49.65
Distribution, %	85.92	10.69	1.85	1.54	100

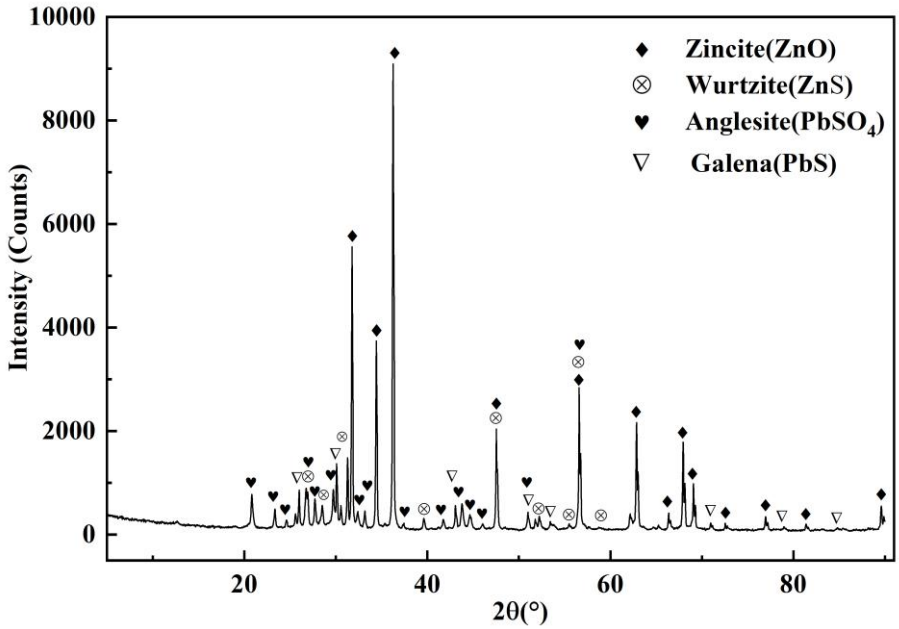

Figure 2. XRD pattern of characterization of the GCR.

To intuitively understand the micromorphology and element composition of GCR, SEM-EDS analysis was carried out, as shown in Figure 3. The microstructure of the raw material is spherical, acicular, cubic and flocculent aggregates. The main constituent elements are Zn, Pb, O, S, Si, Al and Fe. To know the chemical composition of the four typical structures, the five regions (spot. 1–5 in Figure 3a) were analyzed by EDS [34]. Due to the low Ge content in GCR, a scanning electron microscope cannot detect the Ge content. According to the analysis results in Figure 3a and Table 3, the following conclusions can be drawn: spot 1 is a cubic structure, which is a mixture of $PbSO_4$ and PbS, with a small amount of ZnO and ZnS embedded; spot 2 is a spherical structure, which is ZnO, with a small amount of ZnS, $PbSO_4$, PbS, Fe oxide and aluminosilicate embedded. Spot 3 is a flocculent structure, which is mainly composed of ZnO wrapped ZnS mixed particles; spot 4 is an acicular structure, which is composed of high content of ZnO and low content of

ZnS, $PbSO_4$ and PbS; spot 5 is a spherical structure, which is composed of high content of ZnO and low content of ZnS, $PbSO_4$, PbS and SiO_2.

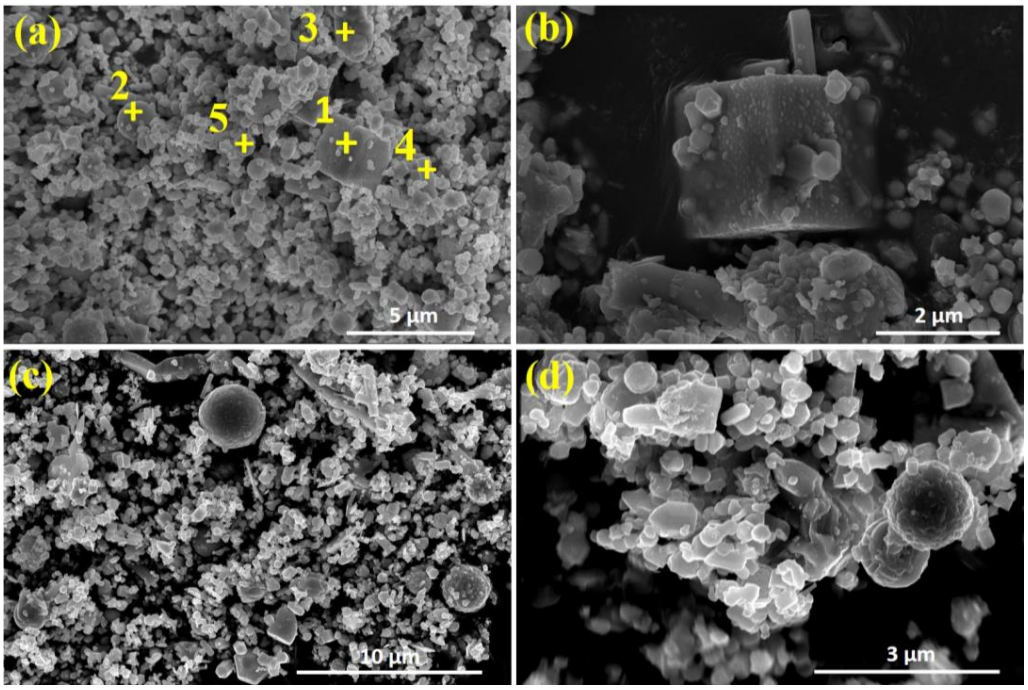

Figure 3. SEM image and EDS analysis areas of the GCR.

Table 3. The EDS analysis results of the selected area of the raw material sample GCR in Figure 3a.

Item	Spot 1		Spot 2		Spot 3		Spot 4		Spot 5	
	wt.%	at.%	wt.%	at.%	wt.%	at.%	wt.%	at.%	wt.%	at.%
Zn	12.24	11.1	46.74	25.09	65.12	32.50	60.41	35.14	63.86	36.86
Pb	64.01	18.31	9.25	1.57	0.00	0.00	11.31	2.07	8.20	1.49
O	14.39	53.3	21.56	47.29	31.34	63.90	24.57	58.39	24.21	57.09
S	9.36	17.3	2.52	2.76	3.54	3.60	3.71	4.40	2.84	3.34
Si	0.00	0.00	9.56	11.95	0.00	0.00	0.00	0.00	0.90	1.21
Al	0.00	0.00	7.17	9.33	0.00	0.00	0.00	0.00	0.00	0.00
Fe	0.00	0.00	3.18	2.00	0.00	0.00	0.00	0.00	0.00	0.00

Therefore, EDS analysis shows that the spherical particles are mainly the mixture of Zn oxide and Pb–Zn oxide, the cubic particles are PbS phase, and the flocculent and acicular particles are mostly ZnO phase. In general, the results of SEM-EDS analysis are consistent with those of Tables 1 and 2 and XRD analysis.

Figure 4 shows BSE (Backscatter electron) image (a) and EPMA element analysis diagrams (b-h) of the GCR. The bright regions in Figure 4b–h correspond to the positions of Zn, Pb, O, S, Si, Fe and Ge, respectively, and the distribution of elements confirms that the main elements of the GCR are Zn, Pb and S. From Figure 4b–h, it can be found that the positions of Zn, Pb, O and S are almost overlapped, which indicates that the phases of GCR may be ZnS, ZnO, $PbSO_4$ and PbS. Similarly, the distributions of O and Si elements in regions 1 and 3 and regions 2 and 4 in Figure 4d,f are highly consistent, indicating that this region is an oxide of Si; the element distributions of O and Fe in regions 2 and 5 in Figure 4d,g are highly coincident, indicating that the region is an oxide of Fe. Due to the low Ge content, the electron probe cannot detect the obvious enriched region of Ge, so it is speculated that the Ge in the GCR may be dispersed in the phases containing Zn, Pb, Si and Fe according to Figure 4h. Therefore, the results of EPMA are consistent with those of XRD and SEM-EDS.

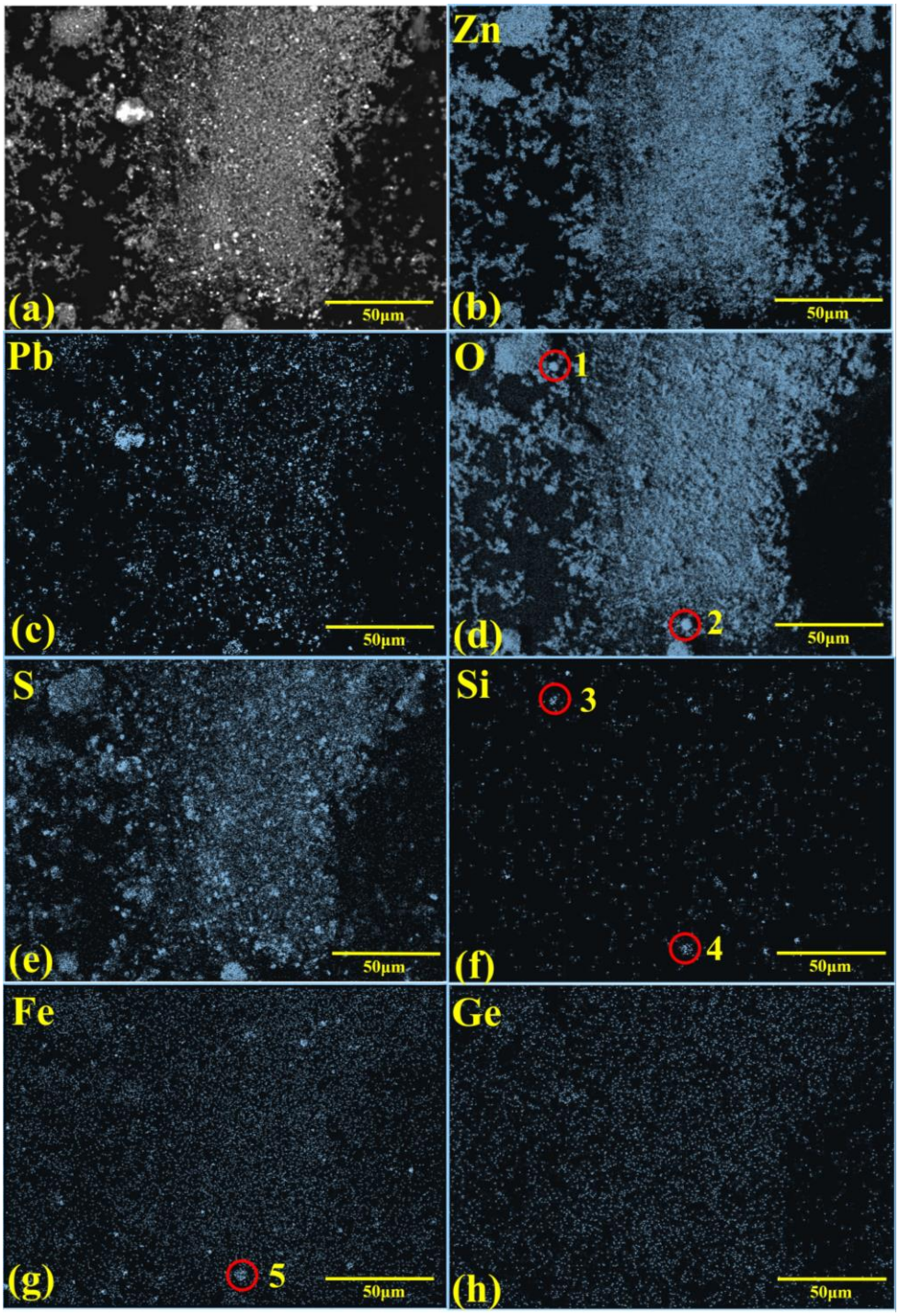

Figure 4. BSE image (**a**) and EPMA elemental images (**b**–**h**) of GCR.

In conclusion, through chemical analysis, XRD analysis, SEM-EDS analysis and EPMA analysis, it is concluded that the main phases of GCR are ZnO, ZnS, $PbSO_4$, PbS, Fe oxides, Si oxides and Al oxides.

3.2. Atmospheric Leaching Experiment

To study the reasons for the low leaching rates of Zn and Ge in GCR leaching under normal pressure and to explore the best reaction conditions, atmospheric leaching experiments were carried out on GCR. The effects of L/S mass ratio, leaching time, initial acidity and temperature on the leaching rate of Zn and Ge are shown in Figures 5–9. With reference to the actual process conditions of the enterprise and the research conditions of others.

is a reference, not a use. is a reference, not a use.The leaching temperature is generally 50–100 °C, the initial acidity is about 160 g·L^{-1}, the L/S mass ratio is 4–7:1, and the leaching time is about 60 min [9,35]. To match the enterprise and existing research, the range of the research parameter value is selected as L/S mass ratio 4–8:1, the leaching temperature is 50–90 °C, and the initial acidity is about 100–200 g·L^{-1}. The time is 30–240 min. According to Section 3.1, the main chemical composition of the GCR is known, so the main reaction of the GCR in sulfuric acid system is as follows.

$$ZnO + H_2SO_4 = ZnSO_4 + H_2O \quad (2)$$

$$GeO + H_2SO_4 = GeSO_4 + H_2O \quad (3)$$

$$GeO_2 + 2H_2SO_4 = Ge(SO_4)_2 + 2H_2O \quad (4)$$

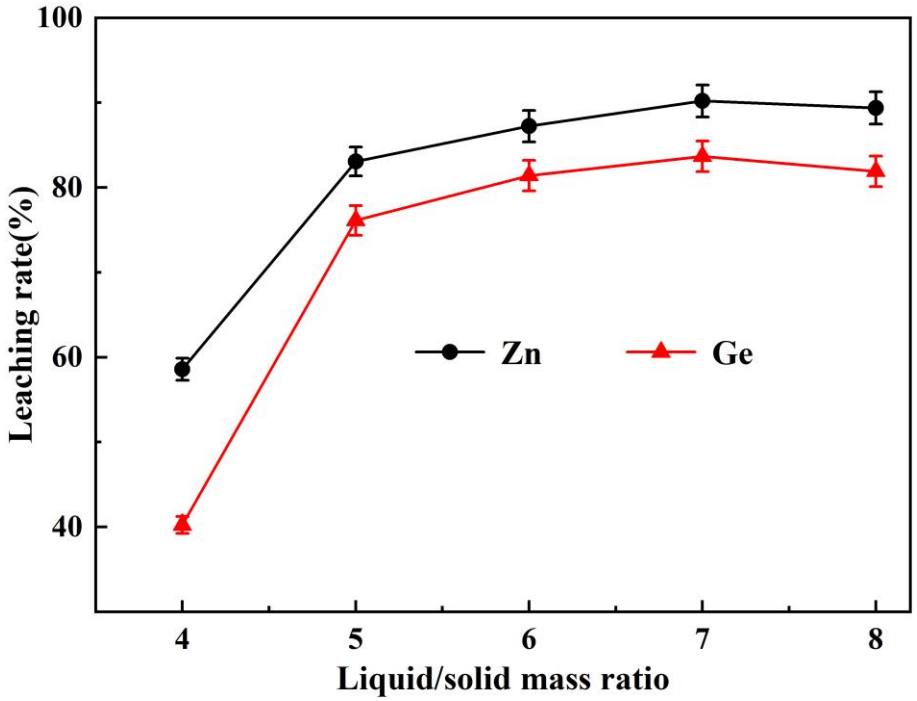

Figure 5. Effect of L/S mass ratio on metal leaching rate (initial acidity = 160 g·L^{-1}, leaching time = 240 min, leaching temperature = 90 °C, and stirring speed = 400 r·min^{-1}).

The leaching rates of Zn and Ge at different L/S mass ratios (4–8:1) are shown in Figure 5. Figure 5 shows that the leaching rates of Zn and Ge increase significantly from 58.58% and 40.22% of 4:1 L/S mass ratio to 89.39% and 81.92% of 8:1 L/S mass ratio, respectively. However, increasing the L/S mass ratio will increase the total content of the leaching agent, resulting in more Fe leaching and increasing the Fe ion concentration in the solution, which will affect the subsequent processing procedures. The φ–pH diagram for a Zn−Fe−H_2O system (a_{Me}^{n+} = 0.01, 25 °C, 1.0 bar) has been depicted using the HSC 6.0 software (Figure 6) [36]. During the experiment, it was found that when L/S mass ratio was 4, 5, and 6, the pH values of the filtrate after the experiment were pH ≥ 5, pH = 1.5–2, and pH ≤ 0.5, respectively. It can be seen from Figure 6 that Fe^{3+} begins to precipitate in the form of $Fe(OH)_3$ at pH ≥ 2.0, which is consistent with previous research results [37–40]. This results in the resorption of free Zn and Ge in solution into the residue by $Fe(OH)_3$. Therefore, the L/S mass ratio was selected as 5:1 in the following experiments.

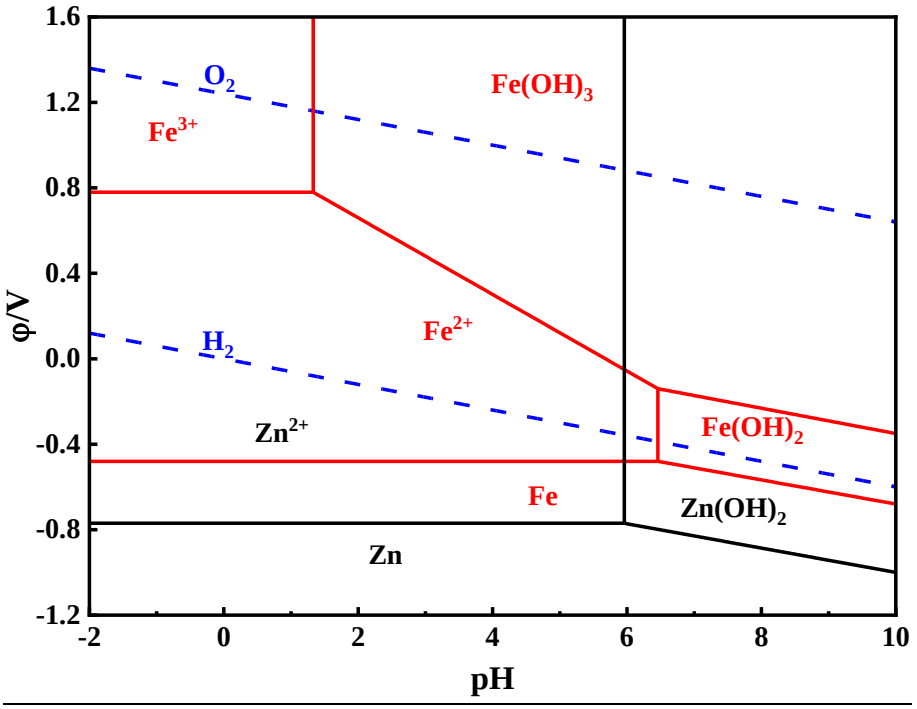

Figure 6. φ−pH diagram for Zn−Fe−H2O system at 25 °C (aMen+ = 0.01, 25 °C, 1.0 bar).

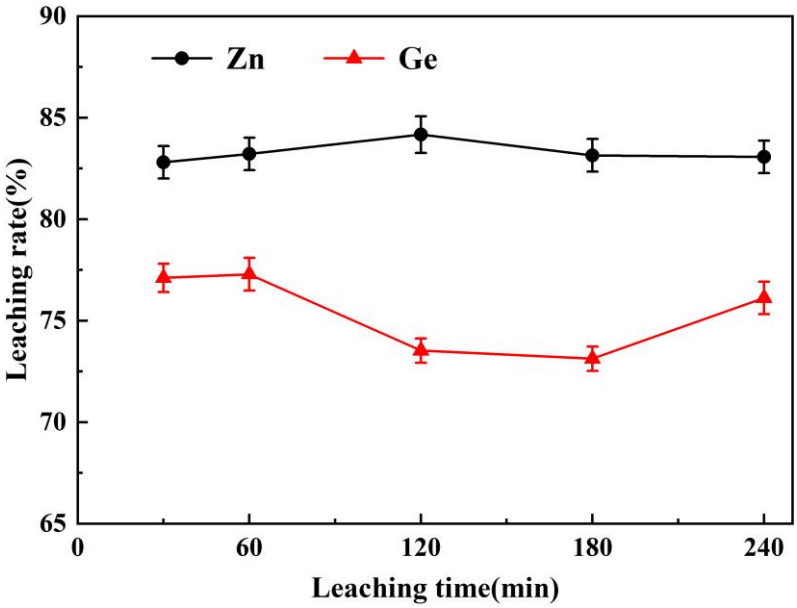

Figure 7. Effect of leaching time on metal leaching rate (L/S mass ratio = 5:1, initial acidity = 160 g·L^{-1}, leaching temperature = 90 °C, and stirring speed = 400 r·min^{-1}).

It can be seen from Figure 7 that the leaching rate of Ge reaches the maximum value of 77.29% in 60 min, and begins to decrease with the increase of time after leaching for 60 min. The leaching rates of Zn first increased and then decreased with the increase of time, but the difference was not significant. This shows that under this method, most of the minerals containing Zn and Ge soluble in sulfuric acid solution can be leached within 60 min. When the leaching experiment continues, other impurity metal minerals may react with sulfuric acid, thereby dissolving the impurity metals into the solution or absorbing and precipitating Zn and Ge in the solution into the residue. Therefore, the best leaching time of GCR is 60 min.

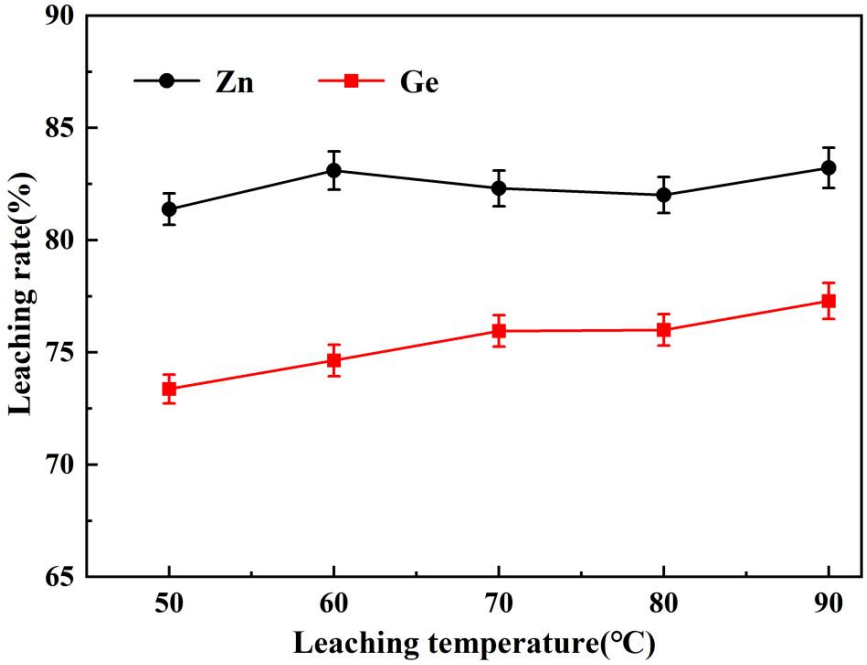

Figure 8. Effect of leaching temperature on metal leaching rate (leaching time = 60 min, initial acidity = 160 g·L^{-1}, L/S mass ratio = 5:1, and stirring speed = 400 r·min^{-1}).

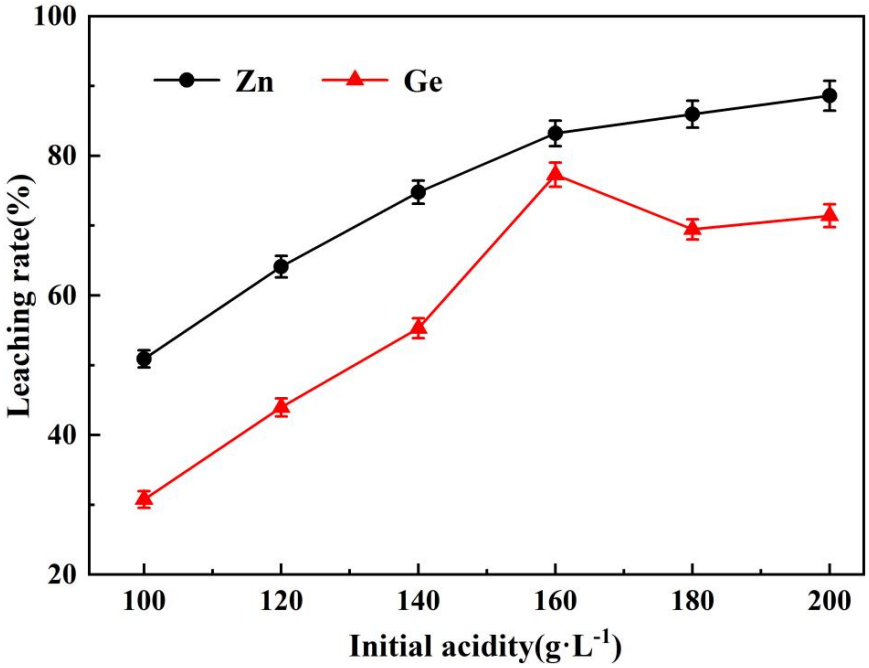

Figure 9. Effect of initial acidity on metal leaching rate (L/S mass ratio = 5:1, leaching time = 60 min, leaching temperature = 90 °C, and stirring speed = 400 r·min^{-1}).

It can be seen from Figure 8 that the leaching rate of Zn increases from 50 °C, decreases slightly at 60 °C and tends to be flat at 90 °C, at which time the leaching rate is 83.22%. The leaching rate of Ge started to increase from 50 °C, and it leveled off at 90 °C, and the leaching rate was 77.29%. During the leaching process, increasing the temperature can effectively ease the binding of mineral particles, promote molecular diffusion and promote the reaction [40]. Therefore, the best leaching temperature of GCR is 90 °C.

The effect of the initial acidity changes from 100 to 200 g·L^{-1} on the leaching rates of Zn and Ge was studied under the conditions of optimal leaching temperature, L/S

mass ratio and leaching time. The results are shown in Figure 9. Figure 9 shows that the concentration of H_2SO_4 has a great influence on the leaching rates of Zn and Ge. This is because when the L/S mass ratio is constant, the sulfuric acid content in the solution will increase with the increase of sulfuric acid concentration, thereby increasing the collision probability of hydrogen ions with compounds and promoting the reaction. However, when the initial acidity increases to 160 $g \cdot L^{-1}$, the leaching rate of Ge reaches the maximum value of 74, and when the initial acidity increases to 180 $g \cdot L^{-1}$, the leaching rate begins to decline. This may be because the solubility of GeO_2 in sulfuric acid decreases with the increase of initial acidity. Therefore, the optimal concentration of H_2SO_4 in this experiment is 160 $g \cdot L^{-1}$.

Based on the above results and analysis and discussion, the best reaction conditions for leaching GCR at atmospheric pressure are: initial acidity of 160 $g \cdot L^{-1}$, L/S mass ratio of 5:1, leaching time of 60 min, and leaching temperature of 90 °C. However, the leaching rates of Zn and Ge were only 83.22% and 77.29% under the optimal pH control conditions.

3.3. Characterization and Analysis of Leaching Residue

The leaching residue obtained after leaching was characterized and analyzed by XRF, XRD, and SEM-EDS. The main chemical composition of the residue is shown in Table 4. Compared with the results in Table 1, the Zn content in Table 4 is significantly reduced, and the Ge content is also reduced, but most of the Ge is still not leached, while the Pb, Si, S and Fe elements are significantly enriched, indicating that the atmospheric leaching process cannot completely leach Ge, nor can it leach sulfide.

Table 4. XRF results of atmospheric leaching residue.

Element	Pb	Zn	S	Fe	Si	Al	As	Ge	Others (e.g., O)
Content, wt.%	35.77	19.00	10.34	6.35	2.24	1.26	1.00	0.03	24.01

XRD analysis of leached residue is shown in Figure 10. Only the diffraction peaks of PbS, ZnS and $PbSO_4$ appear in Figure 10. Compared with Figure 1, the diffraction peaks of ZnO in Figure 10 disappear, but PbS, ZnS and $PbSO_4$ still exist, which indicates that ZnO is easily soluble in sulfuric acid, while PbS and ZnS are difficult to be leached by atmospheric leaching without oxidant.

Figure 11 is a SEM image of the leaching residue. The EDS analysis results of the five points selected in Figure 11 for the leaching residue are shown in Table 5. The structure and shape of the leaching residue are mainly composed of five shapes: sphere, acicular, block, tetragonal and flocculent (marked with numbers 1–5). According to the analysis results in Figure 11, the following conclusions can be drawn: spot 1 is a spherical structure, the main phase of which is ZnS, and contains trace PbS, $PbSO_4$ and SiO_2. Spot 2 is a needle structure, the main phase of which is $PbSO_4$, and contains trace ZnS, PbS, SiO_2 and Fe oxides. Spot 3 is a block structure, the main phase is $PbSO_4$, and contains a small amount of ZnS and PbS; the tetragonal structure of the monomer at spot 4 is mainly composed of $PbSO_4$ particles and contains trace PbS and ZnS; and the flocculent structure of the monomer at spot 5 is mainly composed of $PbSO_4$ and contains trace PbS and ZnS.

According to the SEM-EDS analysis in Figures 3 and 11, Tables 3 and 5, the spherical structure is mainly composed of ZnO particles; the tetragonal structure is mainly composed of Pb sulfate and PbS particles; and the acicular structure is mainly composed of ZnO and ZnS with a small amount of $PbSO_4$ and PbS mixed particles. Compared with Figures 3 and 11, the spherical structure in Figure 11 is reduced, indicating that ZnO has been leached, while the tetragonal structure and acicular structure still exist, indicating that the two phases are difficult to leach. EDS analysis of Table 5 shows that the leaching residue is mainly composed of Zn, Pb, S, O, Fe and Si, which are composed of PbS, ZnS, $PbSO_4$, SiO_2 and Fe oxide. Compared with the previous research results, the above research results are similar in shape, structure and phase of the leaching residue, and the difference is that the Zn content of the

atmospheric leaching residue is higher, which indicates that the atmospheric leaching method is difficult to leach sulfide, thus causing the loss of some Zn. SEM-EDS analysis is consistent with XRD analysis. In summary, $PbSO_4$, PbS, ZnS, SiO_2 and Fe oxides are difficult to leach under atmospheric leaching, which is consistent with the results in Table 4 and Figure 10. This may be one of the main reasons why the leaching rates of Zn and Ge cannot be improved by the atmospheric leaching process.

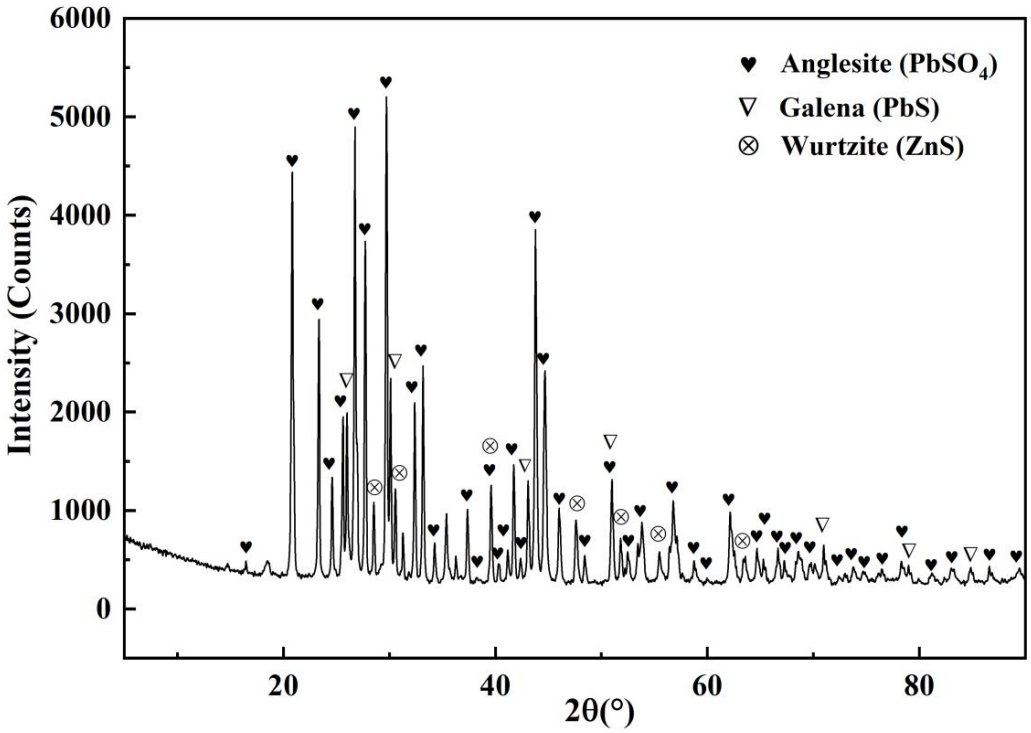

Figure 10. XRD pattern of atmospheric leaching residue (initial acidity = 160 g·L^{-1}, leaching temperature = 90 °C, leaching time = 60 min, and L/S mass ratio = 5:1).

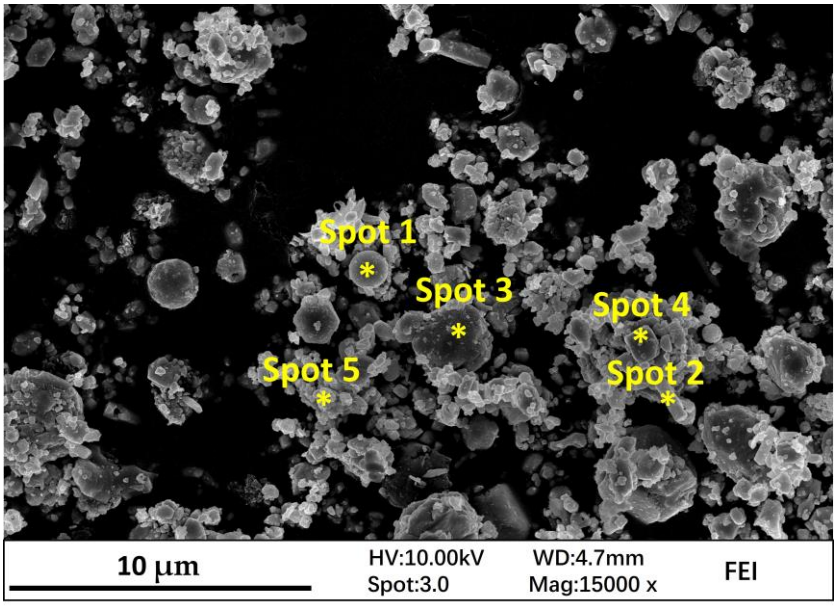

Figure 11. SEM image and EDS analysis areas of atmospheric leaching residue (initial acidity = 160 g·L^{-1}, leaching temperature = 90 °C, leaching time = 60 min, and L/S mass ratio = 5:1).

Table 5. The EDS analysis results of the selected area of atmospheric leaching residue in Figure 11.

Item	Spot 1	Spot 2	Spot 3	Spot 4	Spot 5
	wt.%	wt.%	wt.%	wt.%	wt.%
Zn	59.0	30.4	18.0	6.8	21.5
Pb	19.7	35.4	23.6	68.0	40.6
O	16.7	29.3	51.9	15.1	28.1
S	4.0	4.2	6.4	10.1	9.8
Si	0.6	0.4	0.00	0.00	0.00
Fe	0.00	0.2	0.00	0.00	0.00

Figure 12a,b are the SEM images of the GCR sample and the leaching residue, respectively. From the surface scanning maps, it can be concluded that the brightness and density of Zn and O elements in the leaching residue are significantly lower than those of GCR, while the brightness and density of Pb, S, Si and Fe elements are significantly lower than those of GCR. It is significantly higher than GCR, which indicates that Zn is mostly leached out by atmospheric leaching, while Pb, S, Si and Fe elements are abundantly enriched, indicating that the compounds composed of Pb, S, Si and Fe are more difficult to be leached under conventional conditions. At the same time, the distribution of Pb, O and S in the leaching residue is highly consistent, which proves that the leaching residue contains a large amount of $PbSO_4$. Zn and S, Si, Fe and O have similar distribution characteristics in the leaching residue, which indicates that the leaching residue contains ZnS, SiO_2 and Fe oxides. Due to the low content of Ge, the presence of Ge could not be detected by SEM-EDS. The surface scanning analysis results in Figure 12 show that $PbSO_4$, PbS, ZnS, SiO_2 and Fe oxides are difficult to leaching, which is consistent with the chemical analysis, XRD analysis and SEM-EDS analysis results. According to the research results of Jiang et al., Ge mainly exists in PbS, and it is difficult to leach sulfides by atmospheric leaching without oxidant, which may be the main reason for the low leaching rate of Ge [35].

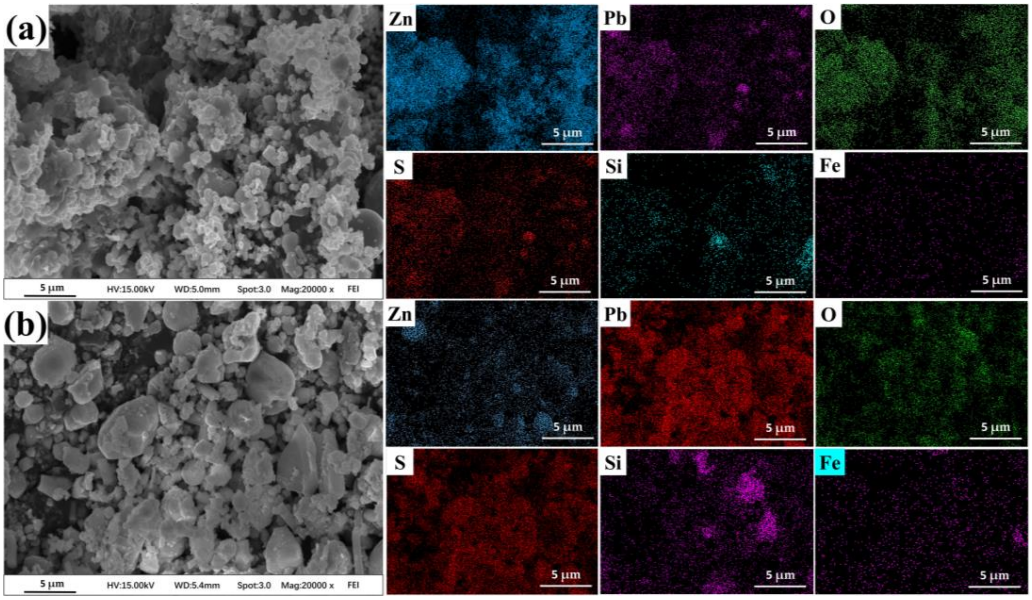

Figure 12. SEM images and EDS mapping: (**a**) the GRC sample; (**b**) the leaching residue (initial acidity = 160 g·L^{-1}, leaching temperature = 90 °C, leaching time = 60 min, and L/S mass ratio = 5:1).

4. Conclusions

According to the research results of this article, the following conclusions can be drawn:

(1) The GCR samples studied in this paper are mainly composed of the following elements: Zn, Pb, S, As, Si, Fe and Ge. XRF, XRD, SEM-EDS and EPMA analysis show that the main phases of GCR are ZnO, ZnS, PbS and $PbSO_4$.

(2) The results of atmospheric leaching experiments show that the best reaction conditions under pH control are: leaching temperature of 90 °C, L/S mass ratio of 5:1, stirring speed of 400 r·min^{-1}, leaching time of 60 min, and initial acidity of 160 g·L^{-1}; under these conditions, the leaching rates of Zn and Ge are 83.22% and 77.29%, respectively. XRD and SEM-EDS show that the leaching residue is mainly composed of ZnS, PbS and $PbSO_4$, and contains a small amount of SiO_2 and Fe oxides.

(3) Ge may be dispersed in ZnO, ZnS, PbS, PbSO4, SiO_2 and Fe oxides. ZnO is easy to be leached by acid, while ZnS and PbS are difficult to be leached by sulfuric acid without oxidant, and SiO_2 and sulfuric acid do not react. This may be one of the main reasons why the atmospheric leaching process cannot increase the Ge leaching rate.

(4) The author believes that under the premise of not increasing the leaching cost and not introducing impurity ions, green and pollution-free oxidants should be added during the leaching process and external field strengthening methods should be introduced to strengthen the leaching of sulfides, such as ultrasonic waves, microwaves, etc., to achieve a low cost, high leaching rate and short leaching process which does not affect the purpose of recovering Zn and Ge in subsequent processes.

Author Contributions: C.X.: Conceptualization, data curation, formal analysis, investigation, methodology and writing—original draft. H.X.: Conceptualization, funding acquisition, resources, software, validation, methodology, writing—review and editing, and supervision. G.J.: Validation, formal analysis, investigation, visualization and writing—original draft. Q.Z.: Validation, data curation, investigation and visualization. L.Z.: Conceptualization, funding acquisition, resources, software, supervision and validation. Y.X.: Validation, data curation, investigation and visualization. All authors have read and agreed to the published version of the manuscript.

Funding: This research was funded by the Yunnan Province basic research special key project (202001AS070009), National Key R&D Program of China (2021YFC2902801), Special fund projects of central government guiding local science and technology development (202107AA110002), Yunnan Xingdian Talent Support Project-Industrial innovation talents (2019-1096), Yunnan Xingdian Talent Support Project- Young talents (2018-73).

Conflicts of Interest: The authors declare that they have no known competing financial interests or personal relationships that could have appeared to influence the work reported in this paper. The authors declare no conflict of interest.

References

1. The Geological Survey of Sweden. Critical Raw Materials. Available online: https://www.sgu.se/en/mineral-resources/critical-raw-materials/ (accessed on 5 September 2022).
2. Ceylan, A.; Rumaiz, A.K.; Caliskan, D.; Ozcan, S.; Ozbay, E.; Woicik, J.C. Effects of rapid thermal annealing on the structural and local atomic properties of ZnO: Ge nanocomposite thin films. *J. Appl. Phys.* **2015**, *117*, 105303. [CrossRef]
3. Depuydt, B.; Theuwis, A.; Romandic, I. Germanium: From the first application of Czochralski crystal growth to large diameter dislocation-free wafers. *Mat. Sci. Semicon. Proc.* **2006**, *9*, 437–443. [CrossRef]
4. Zhang, L.G.; Xu, Z.M. Application of vacuum reduction and chlorinated distillation to enrich and prepare pure germanium from coal fly ash. *J. Hazard. Mater.* **2017**, *321*, 18–27. [CrossRef]
5. Claeys, C.; Simoen, E. Germanium-based technologies: From materials to devices. *Mater. Today* **2007**, *10*, 53.
6. Frenzel, M.; Ketris, M.P.; Gutzmer, J. On the geological availability of germanium. *Miner. Depos.* **2014**, *49*, 471–486. [CrossRef]
7. Seredin, V.V. From coal science to metal production and environmental protection: A new story of success Commentary. *Int. J. Coal Geol.* **2012**, *90*, 1–3. [CrossRef]
8. Dutta, S.K.; Lodhari, D.R. *Extraction of Nuclear and Non-ferrous Metals*; Springer Nature: Berlin/Heidelberg, Germany, 2018.
9. Jiang, T.; Zhang, T.; Liu, Z.H. Pb-based aggregate, Ge-galena coexistence, and Ge-anglesite coprecipitate-Limitations and an improvement of germanium recovery from secondary zinc oxide via H_2SO_4 leaching. *Hydrometallurgy* **2020**, *10*, 5543. [CrossRef]

10. Guo, X.Y.; Yi, Y.; Shi, J.; Tian, Q.H. Leaching behavior of metals from high-arsenic dust by NaOH-Na_2S alkaline leaching. *Trans. Nonferr. Metal. Soc.* **2016**, *26*, 575–580. [CrossRef]
11. Kul, M.; Oskay, K.O.; Şimşir, M.; Sübütay, H.; Kirgezen, H. Optimization of selective leaching of Zn from electric arc furnace steelmaking dust using response surface methodology. *Trans. Nonferr. Metal. Soc.* **2015**, *25*, 2753–2762. [CrossRef]
12. Li, Q.; Rao, X.F.; Xu, B.; Yang, Y.B.; Liu, T.; Jiang, T.; Hu, L. Extraction of manganese and zinc from their compound ore by reductive acid leaching. *Trans. Nonferr. Metal. Soc.* **2017**, *27*, 1172–1179. [CrossRef]
13. Lutandula, M.S.; Kashala, G.N. Zinc oxide production through reprocessing of the electric arc furnace flue dusts. *J. Environ. Chem. Eng.* **2013**, *1*, 600–603. [CrossRef]
14. Ding, W.; Bao, S.X.; Zhang, Y.; Xiao, J.H. Efficient selective extraction of scandium from red mud. *Miner. Process. Extr. Metall. Rev.* **2022**, 1–9. [CrossRef]
15. Liu, F.P.; Liu, Z.H.; Li, Y.H.; Liu, Z.Y.; Li, Q.H.; Zeng, L. Extraction of gallium and germanium from zinc refinery residues by pressure acid leaching. *Hydrometallurgy* **2016**, *64*, 313–320. [CrossRef]
16. Wang, W.K.; Wang, F.C.; Lu, F.H. Microwave alkaline roasting-water dissolving process for germanium extraction from zinc oxide dust and its analysis by response surface methodology (RSM). *Metall. Res. Technol.* **2018**, *115*, 203. [CrossRef]
17. Wei, Q.X.; Yang, C.J.; Chang, J.; Peng, J.H.; Chen, J. Kinetics of microwave roasting of zinc slag oxidation dust with concentrated sulfuric acid and water leaching. *Chem. Eng. Process.* **2015**, *97*, 75–83.
18. Li, M.; Peng, B.; Chai, L.Y.; Peng, N.; Xie, X.D.; Yan, H. Technological mineralogy and environmental activity of zinc leaching residue from zinc hydrometallurgical process. *Trans. Nonferr. Metal. Soc.* **2013**, *23*, 1480–1488. [CrossRef]
19. Min, X.B.; Xie, X.D.; Chai, L.Y.; Liang, Y.J.; Yong, K.E. Environmental availability and ecological risk assessment of heavy metals in zinc leaching residue. *Trans. Nonferr. Metal. Soc.* **2013**, *23*, 208–218. [CrossRef]
20. Chen, B.; Bao, S.X.; Zhang, Y.M.; Ren, L.Y. A novel and sustainable technique to precipitate vanadium from vanadium-rich solutions via efficient ultrasound irradiation. *J. Clean. Prod.* **2022**, *339*, 130755. [CrossRef]
21. Leclerc, N.; Meux, E.; Lecuire, J.M. Hydrometallurgical extraction of zinc from zinc ferrites. *Hydrometallurgy* **2003**, *70*, 175–183. [CrossRef]
22. Antrekowitsch, J.; Antrekowitsch, H. Hydro-metallurgically recovering zinc from electric arc furnace dusts. *JOM* **2001**, *53*, 26–28. [CrossRef]
23. Oustadakis, P.; Tsakiridis, P.E.; Katsiapi, A.; Agatzini-Leonardou, S. Hydrometallurgical process for zinc recovery from electric arc furnace dust (EAFD). Part I: Characterization and leaching by diluted sulphuric acid. *J. Hazard. Mater.* **2010**, *179*, 1–7. [CrossRef] [PubMed]
24. Pickles, C.A. Thermodynamic modelling of the formation of zinc-manganese ferrite spinel in electric arc furnace dust. *J. Hazard. Mater.* **2010**, *179*, 309–317. [CrossRef] [PubMed]
25. Orhan, G. Leaching and cementation of heavy metals from electric arc furnace dust in alkaline medium. *Hydrometallurgy* **2005**, *78*, 236–245. [CrossRef]
26. Takahiro, M.; Romcha, T.C.F.; Katsuy, A.M.; Nagasaka, T. Hydrometallurgical extraction of zinc from CaO treated EAF dust in ammonium chloride solution. *J. Hazard. Mater.* **2016**, *302*, 90–96.
27. Liang, D.; Wang, J.; Wang, Y. Germanium recovery by co-precipitation of germanium and iron in conventional zinc metallurgy. *J. S. Afr. Inst. Min. Metall.* **2008**, *108*, 715–771.
28. Liu, F.P.; Liu, Z.H.; Li, Y.H. Recovery and separation of gallium(III) and germanium(IV) from zinc refinery residues: Part I: Leaching and iron(III) removal. *Hydrometallurgy* **2017**, *169*, 564–570. [CrossRef]
29. Zhang, T.; Jiang, T.; Liu, Z. Recovery of Ge(IV) from synthetic leaching solution of secondary zinc oxide by solvent extraction using tertiary amine (N235) as extractant and trioctyl phosphate (TOP) as modifier. *Miner. Eng.* **2019**, *136*, 155–160. [CrossRef]
30. Zhang, F.; Wei, C.; Deng, Z.G.; Li, C.X.; Li, X.B.; Li, M.T. Reductive leaching of zinc and indium from industrial zinc ferrite particulates in sulphuric acid medi. *Trans. Nonferr. Metal. Soc.* **2016**, *26*, 2495–2501. [CrossRef]
31. Ding, W.; Bao, S.X.; Zhang, Y.; Xiao, J.H. Mechanism and kinetics study on ultrasound assisted leaching of gallium and zinc from corundum flue dust. *Miner. Eng.* **2022**, *183*, 107624. [CrossRef]
32. Chen, B.; Bao, S.X.; Zhang, Y.M. Synergetic strengthening mechanism of ultrasound combined with calcium fluoride towards vanadium extraction from low-grade vanadium-bearing shale. *Int. J. Min. Sci. Technol.* **2021**, *31*, 1095–1106. [CrossRef]
33. Xin, C.F.; Xia, H.Y.; Zhang, Q.; Zhang, L.B.; Zhang, W. Leaching of zinc and germanium from zinc oxide dust in sulfuric acid-ozone media. *Arab. J. Chem.* **2021**, *14*, 103450. [CrossRef]
34. Xin, C.F.; Xia, H.Y.; Jiang, G.Y.; Zhang, Q.; Zhang, L.B.; Xu, Y.J.; Cai, W.C. Mechanism and kinetics study on ultrasonic combined with oxygen enhanced leaching of zinc and germanium from germanium-containing slag dust. *Sep. Purif. Technol.* **2022**, 302. [CrossRef]
35. Jiang, T.; Zhang, T.; Ye, F.C.; Liu, Z. Occurrence state and sulfuric-acid leaching behavior of germanium in secondary zinc oxide. *Miner. Eng.* **2019**, *137*, 334–343. [CrossRef]
36. Huang, H.H. The Eh-pH diagram and its advances. *Metals* **2016**, *6*, 23. [CrossRef]
37. Wang, X.; Zhong, Y.W.; Kang, Y.Z.; Gao, J.T.; Guo, Z.C. Promoted acid leaching of Zn from hazardous zinc-containing metallurgical dusts: Focusing on transformation of Zn phases in selective reduction roasting. *Process. Saf. Environ.* **2022**, *163*, 353–361. [CrossRef]

38. Stefánsson, A. Iron(III) Hydrolysis and Solubility at 25 °C. *Environ. Sci. Technol.* **2007**, *41*, 6117–6123. [CrossRef]
39. Lin, H.; Wu, J.; Zhang, H. Degradation of bisphenol a in aqueous solution by a novel electro/Fe^{3+}/peroxydisulfate process. *Sep. Purif. Technol.* **2013**, *117*, 18–23. [CrossRef]
40. Chiou, C.S.; Chen, Y.H.; Chang, C.T.; Chang, C.Y.; Shie, J.L.; Li, Y.S. Photochemical mineralization of di-n-butyl phthalate with H_2O_2/Fe^{3+}. *J. Hazard. Mater.* **2006**, *135*, 344–349. [CrossRef]